



HAL
open science

Minority-spin conducting states in Fe substituted pyrite CoS₂

Anustup Mukherjee, Alaska Subedi

► **To cite this version:**

Anustup Mukherjee, Alaska Subedi. Minority-spin conducting states in Fe substituted pyrite CoS₂. Journal of Physics: Condensed Matter, 2023, 36 (2), pp.025501. 10.1088/1361-648X/acfde9 . hal-04307902

HAL Id: hal-04307902

<https://hal.science/hal-04307902>

Submitted on 26 Nov 2023

HAL is a multi-disciplinary open access archive for the deposit and dissemination of scientific research documents, whether they are published or not. The documents may come from teaching and research institutions in France or abroad, or from public or private research centers.

L'archive ouverte pluridisciplinaire **HAL**, est destinée au dépôt et à la diffusion de documents scientifiques de niveau recherche, publiés ou non, émanant des établissements d'enseignement et de recherche français ou étrangers, des laboratoires publics ou privés.

Minority-spin conducting states in Fe substituted pyrite CoS_2

Anustup Mukherjee and Alaska Subedi

CPHT, CNRS, École Polytechnique, Institut Polytechnique de Paris, 91128 Palaiseau, France

(Dated: May 8, 2023)

There has been a longstanding debate whether the pyrite CoS_2 or its alloys with FeS_2 are half metallic. We argue using first principles calculations that there is a finite occupation of minority-spin states at the Fermi level throughout the series $\text{Co}_{1-x}\text{Fe}_x\text{S}_2$. Although the exchange-correlation functional influences the specifics of the electronic structure, we observe a similar trend with increasing Fe concentration in both LDA and GGA calculations. Specifically, even as band filling is decreased through Fe substitution, the lowest-lying conduction band in the minority-spin channel broadens such that these states keep getting lowered relative to the Fermi level, which is contrary to the expectations from a rigid band picture. Furthermore, the exchange splitting decreases as more Co atoms are replaced by Fe, and this again brings the minority-spin states closer to the Fermi level. These two mechanisms, in conjunction with the experimental observation that minority-spin bands cross the Fermi level in stoichiometric CoS_2 , indicate that minority-spin charge carriers will always be present in $\text{Co}_{1-x}\text{Fe}_x\text{S}_2$.

I. INTRODUCTION

The pyrite CoS_2 and related alloys $\text{Co}_{1-x}\text{Fe}_x\text{S}_2$ have been extensively investigated due to their possible half-metallic behavior [1]. This was motivated by the observation of Jarrett *et al.* that $\text{Co}_{1-x}\text{Fe}_x\text{S}_2$ is ferromagnetic with a saturation magnetization $M_s \sim 1\mu_B/\text{Co}$ throughout the series $0 \leq x \leq 0.9$ [2]. However, there is a strong debate whether the electronic states at the Fermi level exhibit full spin polarization in these compounds. First principles calculations within the local density approximation (LDA) by Zhao *et al.* find a small minority-spin electron pocket in CoS_2 [3], making this material almost, but not quite, half metallic. On the other hand, calculations within the generalized gradient approximation (GGA) by Shishidou *et al.* show the states at the Fermi level are fully spin-polarized in CoS_2 [4]. Reflectivity measurements and de Haas-van Alphen experiments suggest that the minority-spin pocket is unoccupied [5, 6]. In contrast, point-contact Andreev reflection (PCAR) experiments find a spin polarization P of only 64% [7, 8]. Polarized neutron diffraction experiments show that occupancy of the minority-spin e_g states is required to describe the magnetization distribution in the ferromagnetic phase [9]. Photoemission spectra also suggest that some minority-spin e_g states lie below the Fermi level [10], and this has been confirmed by subsequent angle resolved photoemission spectroscopy (ARPES) experiments [11–13].

Although pure CoS_2 may not be half metallic, Mazin has argued using density functional calculations that $\text{Co}_{1-x}\text{Fe}_x\text{S}_2$ should exhibit half metallicity that is robust to crystallographic disorder for concentrations $0.10 \lesssim x \lesssim 0.75$ [14]. This is because the exchange splitting of the Co e_g states is large, and the gain in Hund energy should be greater than the cost of kinetic energy when only the majority-spin Co e_g states are occupied as electrons are removed through Fe substitution. Indeed, experiments find that the total magnetization increases from a value of $M_s \approx 0.85\mu_B/\text{Co}$ for $x = 0$ to the integral

value of $1\mu_B/\text{Co}$ for $x \approx 0.1$ and maintains this value until $x \approx 0.5$ – 0.6 , before decreasing again as Fe concentration is increased [2, 15–17]. However, PCAR experiments by Cheng *et al.* on samples with $0.35 \leq x \leq 0.9$ show P of only 47–61% even when $M_s = 1\mu_B/\text{Co}$, and those by Wang *et al.* find a maximum P of 85% for $x = 0.15$ [16, 17]. The lack of full spin polarization is inconsistent with the results of most density functional calculations that consider the same levels of Fe substitution [14–16, 18], although one study using the supercell approach does find that minority-spin states are occupied within the GGA [19]. On a related note, we point out that a recent first principles study finds that hole-doped FeS_2 may exhibit full spin-polarization at the Fermi level [20].

In this paper, we reexamine the robustness of half metallicity in $\text{Co}_{1-x}\text{Fe}_x\text{S}_2$ using density functional calculations for $x = 0, 0.25, 0.5, 0.75, \text{ and } 1$. We find that the details of the electronic structure and magnetism depend on whether one uses the GGA or LDA. However, both approaches find that $\text{Co}_{1-x}\text{Fe}_x\text{S}_2$ is not a half-metal for $x > 0$, and they display a consistent trend of qualitative changes in the electronic structure. As electrons are removed via Fe substitution, the band width of the lowest-lying minority-spin conduction band increases. The dispersive part of the band has predominantly S p antibonding character, suggesting that changes in screening modifies the overlap of antibonding orbitals situated at neighboring S_2^{2-} dimers. When Fe concentration is further increased, the exchange splitting of the conduction manifold comprised of Co e_g and S p antibonding states decreases. Both these effects work to ensure that minority-spin states are always occupied for Fe concentrations $x < 1$. Considering the experimental fact that the lowest-lying conduction band in CoS_2 is occupied in the minority-spin channel, our work implies that $\text{Co}_{1-x}\text{Fe}_x\text{S}_2$ may not be half-metallic for any value of x .

TABLE I. Relaxed metal-sulphur (M -S) and sulphur-sulphur (S-S) bond distances obtained using LDA. We used experimental lattice constants a for the end member compounds CoS_2 and FeS_2 and interpolated ones using Vegard's law for the intermediate compositions. Experimental S-S distances for corresponding compositions are given in the final column.

| Compound | a (Å) | Co-S (Å) | Fe-S (Å) | S-S (Å) | S-S (Å) exp |
|--|----------------|---------------------|---------------------|--------------|---------------|
| CoS_2 | 5.539 [21] | 2.316 | — | 2.191 | 2.12 [22] |
| $\text{Co}_{0.75}\text{Fe}_{0.25}\text{S}_2$ | 5.503 [23] | 2.315, 2.302, 2.309 | 2.269 | 2.168, 2.215 | 2.115 [15] |
| $\text{Co}_{0.5}\text{Fe}_{0.5}\text{S}_2$ | 5.475 | 2.300, 2.308, 2.293 | 2.257, 2.269, 2.266 | 2.250, 2.228 | 2.1 [15] |
| $\text{Co}_{0.25}\text{Fe}_{0.75}\text{S}_2$ | 5.443 | 2.293 | 2.254, 2.265, 2.252 | 2.253, 2.259 | — |
| FeS_2 | 5.407 [18, 24] | — | 2.254 | 2.208 | 2.15 [22, 25] |

II. COMPUTATIONAL DETAILS

We performed first principles calculations within the framework of density functional theory [26, 27] using the Vienna *Ab initio* Simulation package [28–30]. We used both the LDA and GGA scheme of Perdew, Burke, and Ernzerhof [31] to approximate the exchange-correlation functional. A converged basis-set energy cut-off of at least 420 eV and Γ -centered k -point mesh of at least $8 \times 8 \times 8$ were used in the calculations. The energy convergence criterion for the self-consistent cycles was set to 10^{-8} eV. The valence electronic configurations of the pseudopotentials were $3d^8 4s^1$ (Co), $3d^7 4s^1$ (Fe) and $3s^2 3p^4$ (S).

III. STRUCTURAL DETAILS

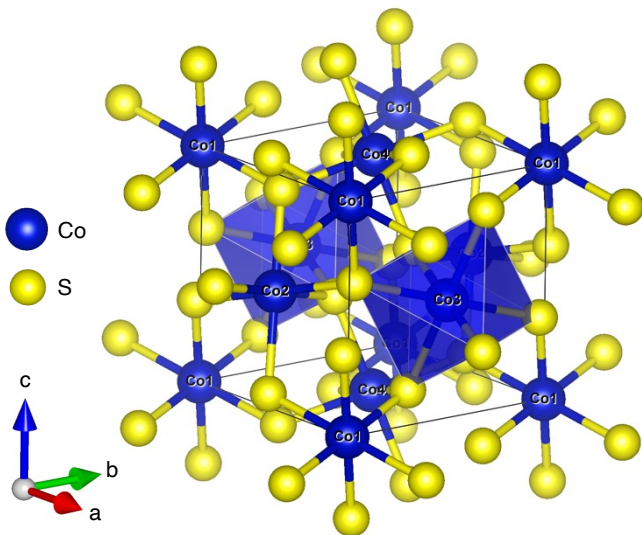


FIG. 1. Structure of the unit cell of pyrite CoS_2 with space group $Pa\bar{3}$. Nearest-neighbor Co-S distances are depicted using solid lines to illustrate the octahedral coordination of Co atoms. There are four formula units in the unit cell. The sites labeled Co1, Co2, Co3, and Co4 are sequentially substituted by Fe to obtain $\text{Co}_{1-x}\text{Fe}_x\text{S}_2$ for $x = 0.25, 0.5, 0.75$, and 1.

Both CoS_2 and FeS_2 occur in the cubic pyrite structure

with space group $Pa\bar{3}$, which is shown in Fig. 1. The unit cell comprises of four Co/Fe atoms at the Wyckoff position $4a$ (0, 0, 0) and eight S atoms at $8c$ (u, u, u), and the respective symmetry-equivalent sites. The Co/Fe atoms are situated inside corner-shared octahedra formed by six dimerized S atoms. Each S atom in the dimer is shared by three octahedra. The only internal parameter u controls the S-S and Co-S distances.

In Fig. 1 we have serially numbered the four Co atoms present in the parent compound. We obtained the five different $\text{Co}_{1-x}\text{Fe}_x\text{S}_2$ compositions for $x = 0, 0.25, 0.5, 0.75$, and 1 considered in the present study by successive replacements of Co atoms. For example, $\text{Co}_{0.75}\text{Fe}_{0.25}\text{S}_2$ ($x = 0.25$) was obtained by substituting Fe at the position Co1, $\text{Co}_{0.5}\text{Fe}_{0.5}\text{S}_2$ ($x = 0.5$) additionally substituting Fe at the position Co2, and so on. We used experimental lattice constant for the end member compounds CoS_2 and FeS_2 [18, 21, 24]. Experiments on intermediate compositions $\text{Co}_{1-x}\text{Fe}_x\text{S}_2$ find that the lattice constant follows the Vegard's law, which we utilize in our study [16, 23]. The internal atomic positions were relaxed for all compositions. For the end member compounds, the Co/Fe-S and S-S distances are parameterized by the internal parameter u , which we find to be 0.3858 and 0.3821 for CoS_2 and FeS_2 , respectively. There are multiple bond distances due to symmetry reduction in the intermediate compounds. The experimental lattice constants and relaxed Co/Fe-S and S-S bond distances over the investigated range of x are given in Table I.

IV. RESULTS AND DISCUSSION

The electronic structure of CoS_2 has previously been studied in detail using DFT calculations [3, 4, 12, 13, 18, 19]. We briefly recapitulate the general features of the non-spin-polarized LDA band structure in the energy range -9 to 3 eV where the S $3p$ and Co $3d$ states responsible for bonding are present. There is a manifold of 20 bands with predominantly S $3p$ character in the energy range -9 to -2.5 eV. Since there are eight S atoms in the unit cell, this implies that two $3p$ orbitals per S are fully filled and one $3p$ orbital per S takes part in the formation of S-S dimers by making a covalent bond. Indeed, the four antibonding S $3p$ bands can be found above

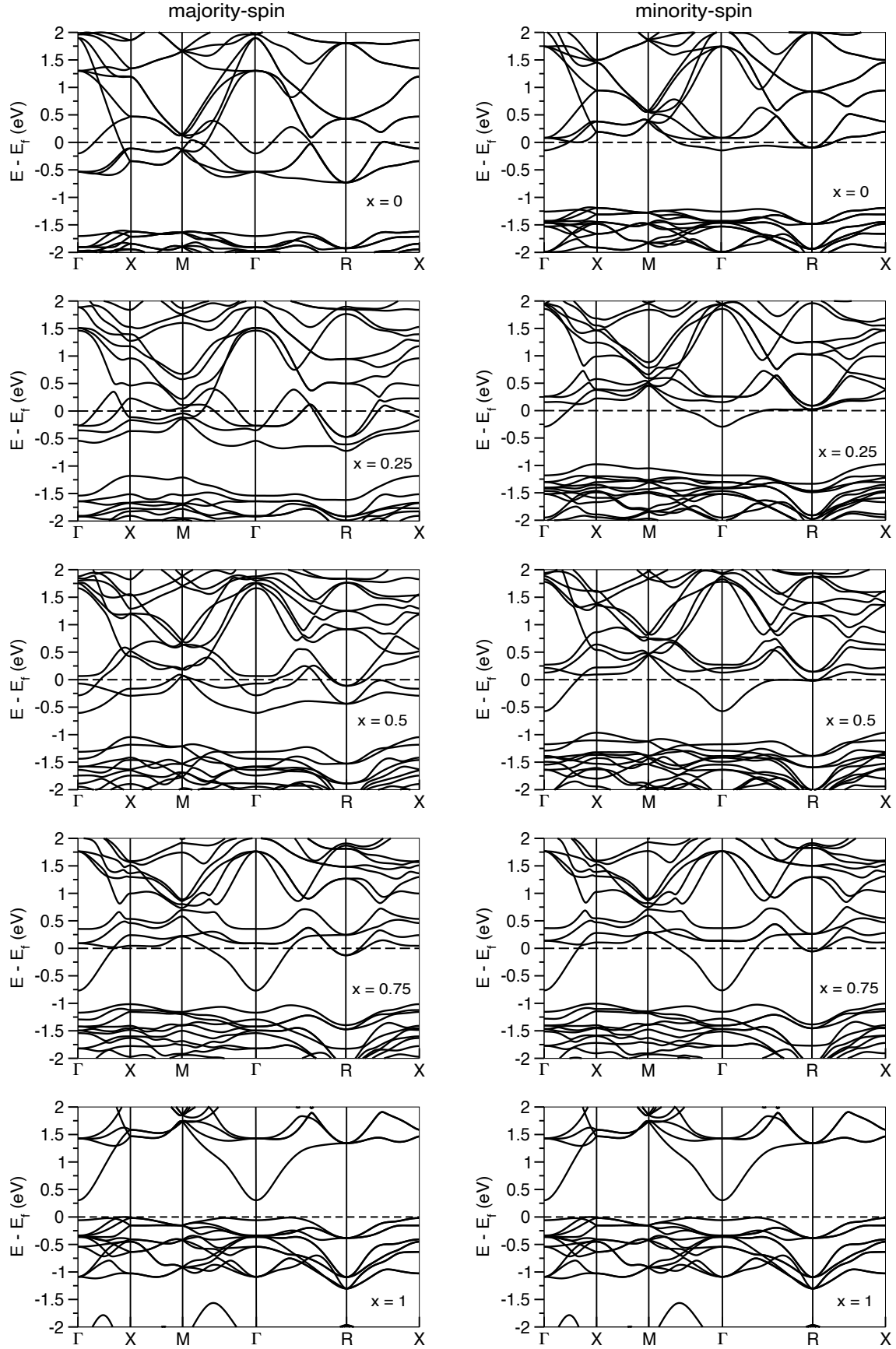


FIG. 2. LDA band structures of $\text{Co}_{1-x}\text{Fe}_x\text{S}_2$ for $x = 0, 0.25, 0.5, 0.75,$ and 1 . The left and right columns show the majority- and minority-spin channels, respectively. The band structure is not spin polarized for FeS_2 ($x = 1$).

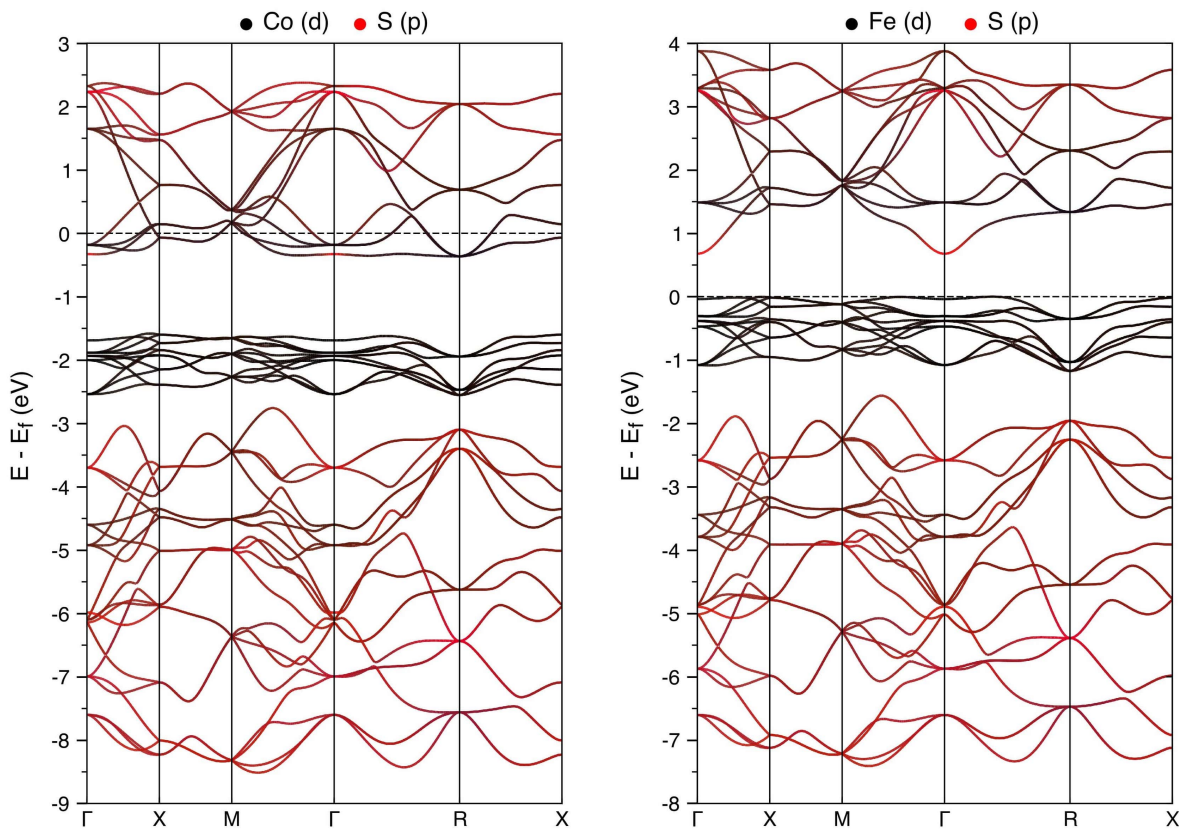


FIG. 3. Non-spin-polarized band structures of CoS_2 (left) and FeS_2 (right). The contribution of Co/Fe $3d$ and S $3p$ characters are depicted by black and red colors, respectively. Both band structures were obtained using the experimental crystal structure of FeS_2 to isolate the effect of chemical substitution.

the Fermi level or partially crossing it. These 20 bands are occupied by a total of 40 electrons, which accounts for the 32 $3p$ electrons of elemental S plus an additional 8 electrons obtained from Co $4s$ orbitals that lie above the Fermi level. This implies nominal valences of Co^{2+} and S_2^{2-} . Just above the S $3p$ states, a manifold of 12 bands with Co t_{2g} character is present in the range -2.5 to -1.1 eV. The Co t_{2g} states are separated from the Co e_g states by a crystal field splitting of around 0.4 eV. The eight Co e_g bands lie in a manifold between -0.7 and 2.5 eV, which is also shared by four antibonding S $3p$ bands. Within this manifold, the low-lying bands carry predominantly Co e_g character while the high-lying ones exhibit mostly S $3p$ character. However, there is intermixing of these states throughout the manifold. In particular, the lowest-lying band in this manifold has significant S $3p$ character near Γ . We also note that S $3p$ bands just below the Co t_{2g} states also show some Co $3d$ character. This indicates significant Co $3d$ -S $3p$ covalency.

We now discuss the evolution of the electronic structure near the Fermi level in the ferromagnetic phase of these compounds as a function of Fe concentration, which is shown in Fig. 2 for the case of LDA. We find that the $x = 0$ compound CoS_2 is not a half metal within LDA, in agreement with previous theoretical [3, 4] and spin-

resolved ARPES [13] study. Our calculations using relaxed atomic positions find minority-spin electron pockets around both the Γ $(0, 0, 0)$ and R $(\frac{1}{2}, \frac{1}{2}, \frac{1}{2})$ points. This differs from early LDA results that only find the pocket around R [3, 4], but agrees with the recent ARPES results [11, 13].

The band structure of $\text{Co}_{0.75}\text{Fe}_{0.25}\text{S}_2$ exhibits band splittings expected from lowering of symmetry due to Fe substitution. However, the structure of bands that cross the Fermi level in the two spin channels changes more than that expected from a simple downward shift of the Fermi level due to hole doping. In particular, the lowest-lying minority-spin conduction band becomes more dispersive around Γ and dips further below the Fermi level. This band has mostly S $3p$ character, and its dispersion increases as Fe concentration is increased. The exchange splitting also decreases as more Co ions are replaced by Fe. As a result the lowest-lying minority-spin band always crosses the Fermi level until all bands in the conduction manifold consisting of Co e_g and S $3p$ antibonding states become unoccupied for FeS_2 .

To understand the reason behind the increased dispersion of the lowest-lying minority-spin conduction band as a function of Fe concentration, we examined the band structures of CoS_2 and FeS_2 calculated using the exper-

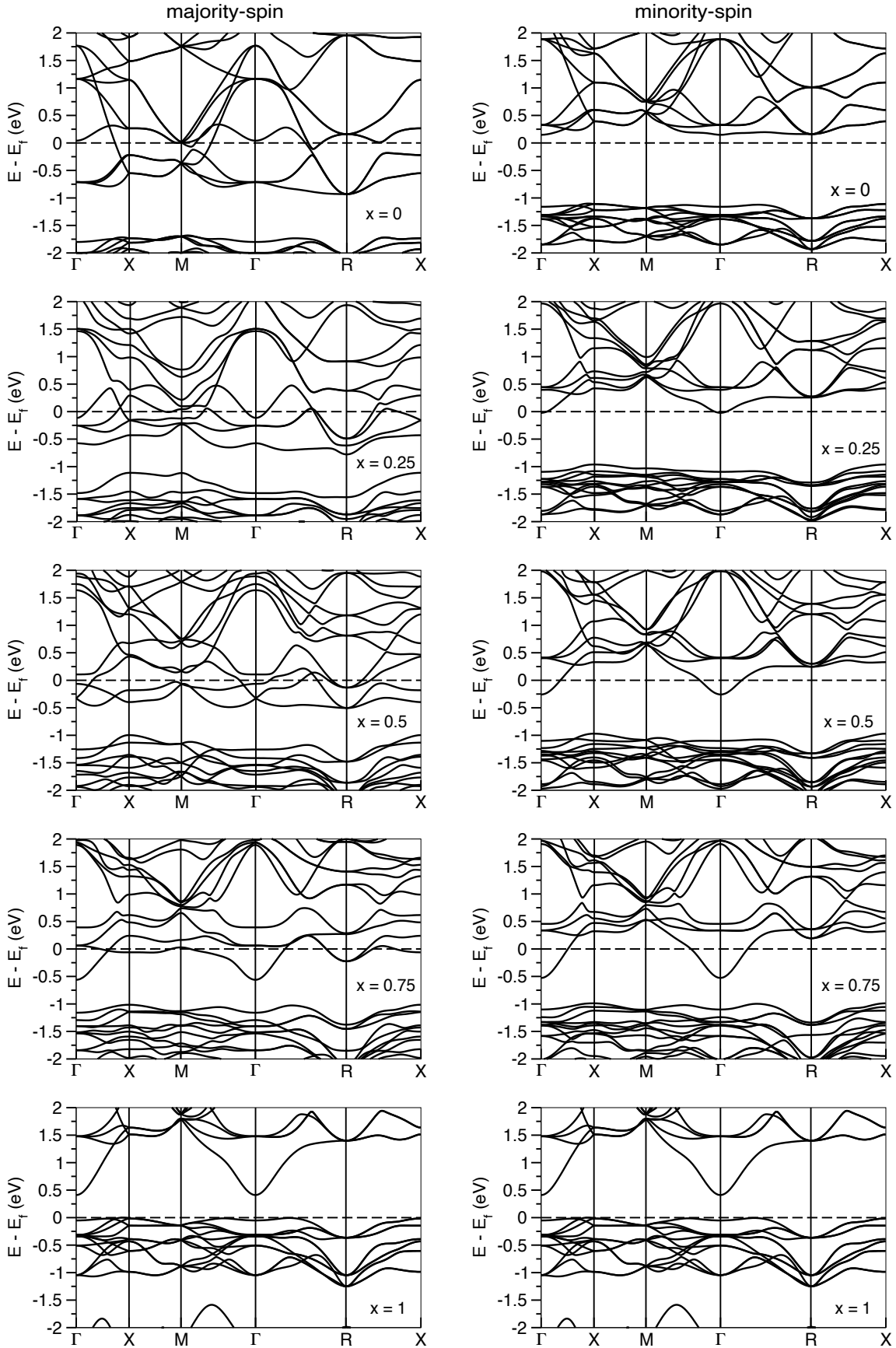


FIG. 4. GGA band structures of $\text{Co}_{1-x}\text{Fe}_x\text{S}_2$ for $x = 0, 0.25, 0.5, 0.75,$ and 1 . The left and right columns show the majority- and minority-spin channels, respectively. The band structure of non-spin-polarized FeS_2 ($x = 1$) is shown for comparison.

imental lattice constant and atomic positions of the latter compound. The result is shown in Fig. 3. We find that the band widths of the occupied S $3p$ and Co t_{2g} manifolds are comparable in the two compounds, with values of ~ 6 and ~ 1 eV, respectively. However, the band width of the mixed Co e_g and S $3p$ antibonding manifold is 2.7 eV in CoS_2 and 3.2 eV in FeS_2 . The increase in the band width is mostly due to the larger dispersion of the lowest- and highest-lying bands in the conduction manifold, which have mostly S $3p$ antibonding character. Since this dispersion describes the overlap of the antibonding orbitals residing on neighboring S_2^{2-} dimers, the reduced band width in CoS_2 indicates that hopping through the dimers is reduced due to screening of the orbitals when the occupation of S $3p$ antibonding states is increased. The reduced covalency due to increased band filling is also evident in the smaller distances from the midpoint of the S $3p$ manifold to the midpoints of the Co t_{2g} and mixed Co e_g /S $3p$ antibonding manifolds in CoS_2 .

Band structures of the five compounds calculated using the GGA functional, which are shown in Fig. 4, also display similar increase of the width of the S $3p$ antibonding bands that leads to the occupancy of minority-spin states as Fe concentration is increased. CoS_2 is a half-metal within the GGA, consistent with previous studies [4]. This reflects GGA functional's tendency to overestimate magnetism. As electrons are removed due to Fe substitution in $\text{Co}_{0.75}\text{Fe}_{0.25}\text{S}_2$, the lowest-lying conduction band in the minority-spin channel becomes broader and gets slightly occupied. The band continues to become broader as Fe concentration is increased, and the exchange splitting additionally gets smaller. As a result $\text{Co}_{1-x}\text{Fe}_x\text{S}_2$ is not half-metallic for $x \geq 0.25$.

Table II gives total magnetization M_s/Co obtained using both LDA and PBE for the five compounds that we have considered, and the trend in M_s/Co highlights the role of both broadening of the lowest-lying S $3p$ antibonding band and reduction of the exchange splitting in forestalling the formation of a half-metallic state as Fe concentration is increased. In agreement with the experiments, M_s/Co obtained using LDA increases going from $x = 0$ to 0.25, indicating that the electronic states are more exchange-split in $\text{Co}_{0.75}\text{Fe}_{0.25}\text{S}_2$. This is also evident when one compares the LDA band structures for $x = 0$ and 0.25 in Fig. 2. The flat part of the lowest-lying minority-spin conduction band along Γ - R is below the Fermi level for $x = 0$. However, when this band becomes more dispersive around Γ for $x = 0.25$, the flat part along Γ - R shifts slightly above the Fermi level in the minority-spin channel, which results in an increased value of M_s/Co . Similarly, M_s/Co obtained from PBE decreases by only 0.2% when going from $x = 0$ to 0.25. The corresponding PBE band structures in Fig. 4 again show that the main effect of Fe substitution is to increase the dispersion of the lowest-lying conduction band in the minority channel around Γ , which consists of states with predominantly S $3p$ antibonding character. The broader

S $3p$ antibonding band slightly crosses the Fermi level, once more highlighting that occupation of minority-spin states for $x = 0.25$ occurs due to changes in screening of the S $3p$ antibonding orbitals rather than due to a decrease in exchange splitting. As Fe concentration is further increased, the relative splitting of the conduction manifold in the majority- and minority-spin channels also decreases significantly within both LDA and GGA. This leads to increasing occupation of the minority-spin states, and it gets reflected in the noticeably smaller M_s/Co obtained using both LDA and GGA as x is increased to 0.5 and 0.75. We note that the nonintegral value of M_s/Co we obtain is in contrast to previous calculations that find $M_s/\text{Co} = 1\mu_B$ [15, 16, 23, 32], which is likely caused by the use of experimental internal atomic positions, the DFT+ U method, or fully relaxed lattice parameters. However, experiments [2, 33] do observe a decrease in M_s/Co value for higher Fe concentrations, which is also supported by theoretical results [14].

TABLE II. Magnetic moments per Co of $\text{Co}_{1-x}\text{Fe}_x\text{S}_2$ obtained using LDA and GGA.

| Compound | LDA | PBE |
|--|-----------------------------|-----------------------------|
| | M_s/Co (μ_B) | M_s/Co (μ_B) |
| CoS_2 | 0.720 | 1.0 |
| $\text{Co}_{0.75}\text{Fe}_{0.25}\text{S}_2$ | 0.915 | 0.998 |
| $\text{Co}_{0.5}\text{Fe}_{0.5}\text{S}_2$ | 0.715 | 0.965 |
| $\text{Co}_{0.25}\text{Fe}_{0.75}\text{S}_2$ | 0.179 | 0.803 |
| FeS_2 | – | – |

V. CONCLUSIONS

We investigated the electronic and magnetic properties of $\text{Co}_{1-x}\text{Fe}_x\text{S}_2$ for $x = 0, 0.25, 0.5, 0.75$, and 1 using first principles calculations and showed that this series of compounds does not host a half-metallic phase. The effect of chemical doping was considered by explicit substitution of Co with Fe. We find that the details of the band structure of these compounds obtained using LDA and GGA functionals are different. However, both functionals find that the lowest-lying minority-spin conduction band becomes more dispersive as Fe concentration is increased such that this band remains partially occupied even when the overall band filling is decreased via hole doping. Our band structure calculations for CoS_2 and FeS_2 using the same structural parameters highlight that the increase in band width of the conduction manifold is due to reduced screening of the S $3p$ antibonding states. Furthermore, we find that the exchange splitting between the majority- and minority-spin states decrease for compounds with higher Fe concentrations. As a result, the Fermi level and the bands in the minority-spin channel simultaneously get lowered, and there is a finite occupation of minority-spin states at the Fermi level for

all the nonzero values of Fe concentrations that we studied. Since ARPES experiments show that the lowest-lying minority-spin conduction band crosses the Fermi level even in stoichiometric CoS_2 , the two trends identified in our results indicate that $\text{Co}_{1-x}\text{Fe}_x\text{S}_2$ may not be half metallic for any Fe concentration.

ACKNOWLEDGMENTS

We are thankful to Sylvie Hébert for useful discussions. This work was supported by Agence Nationale de la

Recherche under grant ANR-21-CE50-0033 and GENCI-TGCC under grant A0130913028.

-
- [1] C. Leighton, M. Manno, A. Cady, J. W. Freeland, L. Wang, K. Umemoto, R. M. Wentzcovitch, T. Y. Chen, C. L. Chien, P. L. Kuhns, M. J. R. Hoch, A. P. Reyes, W. G. Moulton, E. D. Dahlberg, J. Checkelsky, and J. Eckert, Composition controlled spin polarization in $\text{Co}_{1-x}\text{Fe}_x\text{S}_2$ alloys, *J. Phys.: Condens. Matter* **19**, 315219 (2007).
- [2] H. S. Jarrett, W. H. Cloud, R. J. Bouchard, S. R. Butler, C. G. Frederick, and J. L. Gillson, Evidence for itinerant d -electron ferromagnetism, *Phys. Rev. Lett.* **21**, 617 (1968).
- [3] G. L. Zhao, J. Callaway, and M. Hayashibara, Electronic structures of iron and cobalt pyrites, *Phys. Rev. B* **48**, 15781 (1993).
- [4] T. Shishidou, A. J. Freeman, and R. Asahi, Effect of GGA on the half-metallicity of the itinerant ferromagnet CoS_2 , *Phys. Rev. B* **64**, 180401 (2001).
- [5] R. Yamamoto, A. Machida, Y. Moritomo, and A. Nakamura, Reconstruction of the electronic structure in half-metallic CoS_2 , *Phys. Rev. B* **59**, R7793 (1999).
- [6] A. Teruya, F. Suzuki, D. Aoki, F. Honda, A. Nakamura, M. Nakashima, Y. Amako, H. Harima, M. Hedo, T. Nakama, *et al.*, Large cyclotron mass and large ordered moment in ferromagnet CoS_2 compared with paramagnet CoSe_2 , *J. Phys. Soc. Jpn.* **85**, 064716 (2016).
- [7] L. Wang, T. Y. Chen, and C. Leighton, Spin-dependent band structure effects and measurement of the spin polarization in the candidate half-metal CoS_2 , *Phys. Rev. B* **69**, 094412 (2004).
- [8] L. Wang, T. Y. Chen, C. L. Chien, and C. Leighton, Sulfur stoichiometry effects in highly spin polarized CoS_2 single crystals, *Appl. Phys. Lett.* **88**, 232509 (2006).
- [9] P. Brown, K.-U. Neumann, A. Simon, F. Ueno, and K. Ziebeck, Magnetization distribution in CoS_2 ; is it a half metallic ferromagnet?, *J. Phys.: Condens. Matter* **17**, 1583 (2005).
- [10] T. Takahashi, Y. Naitoh, T. Sato, T. Kamiyama, K. Yamada, H. Hiraka, Y. Endoh, M. Usuda, and N. Hamada, Para- to ferromagnetic phase transition of CoS_2 studied by high-resolution photoemission spectroscopy, *Phys. Rev. B* **63**, 094415 (2001).
- [11] N. Wu, Y. B. Losovyj, D. Wisbey, K. Belashchenko, M. Manno, L. Wang, C. Leighton, and P. A. Dowben, The electronic band structure of CoS_2 , *J. Phys.: Condens. Matter* **19**, 156224 (2007).
- [12] N. B. M. Schröter, I. Robredo, S. Klemenz, R. J. Kirby, J. A. Krieger, D. Pei, T. Yu, S. Stolz, T. Schmitt, P. Dudin, T. K. Kim, C. Cacho, A. Schnyder, A. Bergara, V. N. Strocov, F. de Juan, M. G. Vergniory, and L. M. Schoop, Weyl fermions, fermi arcs, and minority-spin carriers in ferromagnetic CoS_2 , *Sci. Adv.* **6**, eabd5000 (2020).
- [13] H. Fujiwara, K. Terashima, J. Otsuki, N. Takemori, H. O. Jeschke, T. Wakita, Y. Yano, W. Hosoda, N. Kataoka, A. Teruya, M. Kakihana, M. Hedo, T. Nakama, Y. Ōnuki, K. Yaji, A. Harasawa, K. Kuroda, S. Shin, K. Horiba, H. Kumigashira, Y. Muraoka, and T. Yokoya, Anomalously large spin-dependent electron correlation in the nearly half-metallic ferromagnet CoS_2 , *Phys. Rev. B* **106**, 085114 (2022).
- [14] I. I. Mazin, Robust half metallicity in $\text{Fe}_x\text{Co}_{1-x}\text{S}_2$, *Appl. Phys. Lett.* **77**, 3000 (2000).
- [15] K. Ramesha, R. Seshadri, C. Ederer, T. He, and M. A. Subramanian, Experimental and computational investigation of structure and magnetism in pyrite $\text{Co}_{1-x}\text{Fe}_x\text{S}_2$: Chemical bonding and half-metallicity, *Phys. Rev. B* **70**, 214409 (2004).
- [16] L. Wang, K. Umemoto, R. M. Wentzcovitch, T. Y. Chen, C. L. Chien, J. G. Checkelsky, J. C. Eckert, E. D. Dahlberg, and C. Leighton, $\text{Co}_{1-x}\text{Fe}_x\text{S}_2$: A tunable source of highly spin-polarized electrons, *Phys. Rev. Lett.* **94**, 056602 (2005).
- [17] L. Wang, T. Y. Chen, C. L. Chien, J. G. Checkelsky, J. C. Eckert, E. D. Dahlberg, K. Umemoto, R. M. Wentzcovitch, and C. Leighton, Composition controlled spin polarization in $\text{Co}_{1-x}\text{Fe}_x\text{S}_2$: Electronic, magnetic, and thermodynamic properties, *Phys. Rev. B* **73**, 144402 (2006).
- [18] K. Umemoto, R. M. Wentzcovitch, L. Wang, and C. Leighton, Electronic structure of $\text{Co}_{1-x}\text{Fe}_x\text{S}_2$, *Phys. Status Solidi b* **243**, 2117 (2006).
- [19] Z.-Y. Feng, Y. Yang, and J.-M. Zhang, The structural, electronic and magnetic properties of $\text{Co}_{1-x}\text{Fe}_x\text{S}_2$, *Mater. Res. Express* **5**, 016507 (2018).
- [20] B.-H. Lei and D. J. Singh, Ferromagnetism in a semiconductor with mobile carriers via low-level nonmagnetic doping, *Phys. Rev. Appl.* **15**, 044036 (2021).
- [21] S. Hébert, E. Guilmeau, D. Berthebaud, O. I. Lebedev, V. Roddatis, and A. Maignan, Transport and magnetic properties of highly densified CoS_2 ceramic, *J. Appl. Phys* **114**, 103703 (2013).

- [22] E. Nowack, D. Schwarzenbach, and T. Hahn, Charge densities in CoS_2 and NiS_2 (pyrite structure), *Acta Crystallogr. Sect. B* **47**, 650 (1991).
- [23] S. F. Cheng, G. T. Woods, K. Bussmann, I. I. Mazin, R. J. Soulen, E. E. Carpenter, B. N. Das, and P. Lubitz, Growth and magnetic properties of single crystal $\text{Fe}_{1-x}\text{Co}_x\text{S}_2$ ($x = 0.35 - 1$), *J. Appl. Phys.* **93**, 6847 (2003).
- [24] R. W. G. Wyckoff, *Crystal Structures - Volume 1*. (New York: Interscience., 1963).
- [25] S. L. Finklea III, L. Cathey, and E. L. Amma, Investigation of the bonding mechanism in pyrite using the mössbauer effect and x-ray crystallography, *Acta Crystallogr. A* **32**, 529 (1976).
- [26] P. Hohenberg and W. Kohn, Inhomogeneous electron gas, *Phys. Rev.* **136**, B864 (1964).
- [27] W. Kohn and L. J. Sham, Self-consistent equations including exchange and correlation effects, *Phys. Rev.* **140**, A1133 (1965).
- [28] G. Kresse and J. Hafner, Ab initio molecular dynamics for liquid metals, *Phys. Rev. B* **47**, 558 (1993).
- [29] G. Kresse and J. Furthmüller, Efficiency of ab-initio total energy calculations for metals and semiconductors using a plane-wave basis set, *Comput. Mat. Sci.* **6**, 15 (1996).
- [30] G. Kresse and J. Furthmüller, Efficient iterative schemes for ab initio total-energy calculations using a plane-wave basis set, *Phys. Rev. B* **54**, 11169 (1996).
- [31] J. P. Perdew, K. Burke, and M. Ernzerhof, Generalized gradient approximation made simple, *Phys. Rev. Lett.* **77**, 3865 (1996).
- [32] E. Day-Roberts, T. Birol, and R. M. Fernandes, Contrasting ferromagnetism in pyrite FeS_2 induced by chemical doping versus electrostatic gating, *Phys. Rev. Mater.* **4**, 054405 (2020).
- [33] S. Ogawa, S. Waki, and T. Teranishi, Magnetic and electrical properties of 3d transition-metal disulfides having the pyrite structure, *Int. J. Magn.* **5**, 349 (1974).